J. Comp. Path. 2014, Vol. 150, 325–331

Available online at www.sciencedirect.com

ScienceDirect

ELSEVIER

www.elsevier.com/locate/jcpa

DISEASE IN WILDLIFE OR EXOTIC SPECIES

Ultrastructural Morphogenesis of an Amphibian Iridovirus Isolated from Chinese Giant Salamander (*Andrias davidianus*)

J. Ma, L. Zeng, Y. Zhou, N. Jiang, H. Zhang, Y. Fan, Y. Meng and J. Xu

Division of Fish Disease, Yangtze River Fisheries Research Institute, Chinese Academy of Fishery Sciences; Key Laboratory of Freshwater Biodiversity Conservation, Ministry of Agriculture, Wuhan, Hubei 430223, PR China

Summary

Haemorrhagic disease of Chinese giant salamanders (*Andrias davidianus*) (CGSs) is an emerging condition caused by an iridovirus of the genus *Ranavirus* within the family Iridoviridae. Several studies have described different biological properties of the virus, but some aspects of its replication cycle, including ultrastructural alterations, remain unknown. The aim of the present study was to describe the morphogenesis of Chinese giant salamander iridovirus (GSIV) in an epithelioma papulosum cyprinid (EPC) cell line at the ultrastructural level. Cells were infected with GSIV at a multiplicity of infection (MOI) of 10 and examined at 1, 2, 4, 6, 12, 24, 48, 72, 84 and 96 h post infection. GSIV entered EPC cells by endocytosis or fusion after adsorption to the cell membrane. Following uncoating, the viral cores translocated to the nucleus and the virus began to replicate. Different stages of virus self-assembly were observed in the slightly electron-lucent viromatrix near the cell nucleus. In the late phase of virus infection, most nucleocapsids were mature and formed a typical icosahedral shape and aggregated in pseudocrystalline array at the viromatrix or were budding at the plasma membrane. Virus infection was readily detected by electron microscopy before cytopathic effect appeared in cell culture. The EPC cell line represents a suitable in-vitro model for study of GSIV morphogenesis and characterization of the GSIV replication cycle.

Keywords: Chinese giant salamander iridovirus (GSIV); electron microscopy; ultrastructural morphogenesis

Introduction

The Chinese giant salamander (*Andrias davidianus*) (CGS), of the family Cryptobranchidae, is the largest extant amphibian species in the world. The CGS population has been declining in number over the past 50 years. The CGS is classified as a critically endangered species by the International Union for Conservation of Nature and Natural Resources and is categorized within class II of the national protected animals in China (Wang *et al*., 2004). The losses of the CGS are results of habitat loss or fragmentation, competition with introduced fish or frogs, harmful effects of pesticides or pollution and infections. Environmental stress can reduce immune defence and make CGSs more susceptible to microbial infections (Chinchar, 2002; Wang *et al*., 2004). In the past 30 years, artificial breeding and farming has been used to protect the CSG in China. Approximately 2 million CGSs are bred in China each year; however, artificial breeding and farming has resulted in the occurrence of many diseases affecting these animals. Recently, a pathogenic virus, the Chinese giant salamander iridovirus (GSIV), has been isolated from CGSs with severe subcutaneous haemorrhage, swelling and ulceration of the limbs, in addition to anaemia, ascites and visceral haemorrhage (Geng *et al*., 2010; Gao *et al*., 2012).

Many iridoviruses are associated with serious systemic diseases in amphibians (Essani and Granoff, 1989; Alves de Matos and Paperna, 1993; Cunningham *et al*., 1993; Hengstberger *et al*., 1993;

Correspondence to: L. Zeng (e-mail: zenglingbing@gmail.com).

0021-9975/$ - see front matter
http://dx.doi.org/10.1016/j.jcpa.2013.09.007

Drury *et al.*, 1995; Zupanovic *et al.*, 1998; Zhang *et al.*, 2001; Geng *et al.*, 2010) and fish (Hedrick *et al.*, 1992; Hedrick and McDowell, 1995; Ahne *et al.*, 1997; Granzow *et al.*, 1997; Watson *et al.*, 1998). The GSIV is a newly identified virus belonging to the family Iridoviridae based on its morphology and DNA genome (Geng *et al.*, 2010). The identification of a new iridovirus isolated from the CGS necessitates further investigation in order to understand the epizootiology of the disease caused by the virus. Previous studies have shown that GSIV is a double-stranded DNA virus with icosahedral symmetry and a diameter of approximately 140 nm. Studies of the ultrastructure and morphogenesis of viruses are requisite for understanding mechanisms of viral infection, the pathogenesis of disease and the development of new vaccines and antiviral treatments. However, there is little known about the morphogenesis of GSIV. The aim of the present study was to investigate the morphogenesis of GSIV in an epithelioma papulosum cyprinid (EPC) cell line, which is known to be susceptible to infection with GSIV (Jiang *et al.*, 2011; Gao *et al.*, 2012).

Materials and Methods

Cells and Virus

The EPC cell line (Fijan *et al.*, 1983) was obtained from the China Center for Type Culture Collection (CCTCC), Wuhan University. EPC cells were grown in 25 cm^2 cell culture flasks at 25°C in Eagle's minimal essential medium (EMEM; Sigma, St Louis, Missouri, USA) supplemented with 10% fetal bovine serum.

The GSIV was isolated in the EPC cell line from an infected CGS in 2010 (Gao *et al.*, 2012; Zhou *et al.*, 2012). The viral titre was determined by the standard 50% tissue culture infective dose ($TCID_{50}$) method (Reed and Muench, 1938).

Growth Curve

A confluent monolayer of EPC cells was infected with GSIV at a multiplicity of infection (MOI) of 10, while the control cells were inoculated with EMEM. The cells were incubated for 1 h at 25°C for adsorption, then supernatants were decanted and 5 ml of maintenance medium with 2% fetal bovine serum was added. Three virus-infected flasks were harvested at 1, 2, 4, 6, 12, 24, 48, 72, 84 and 96 h post inoculation (hpi). All harvested samples were frozen-thawed twice, centrifuged and diluted from 10^{-1} to 10^{-9} in EMEM for $TCID_{50}$/ml determination. Viral titration was performed in EPC cells with six repetitions per dilution. Viral titres were calculated as described by Reed and Muench (1938).

Electron Microscopy

The collected cells were fixed with 2% glutaraldehyde, post-fixed in osmium tetroxide, dehydrated and embedded (Braunwald *et al.*, 1985). Ultrathin sections were cut with a microtome (UC7, Leica, Germany) and stained with uranyl acetate and lead citrate, then examined with a Hitachi H-7650 transmission electron microscope.

Results

Growth Curve of GSIV in EPC Cells

Following infection, a log phase increase in virus production was followed by an eclipse period of about 6 h. Virus production peaked between 48 and 72 hpi (Fig. 1). The GSIV one-step growth is similar to viruses replicating *in vitro* (Furukawa *et al.*, 1973).

Morphogenesis of GSIV

Morphogenesis of GSIV in EPC cells showed four steps: entry of virus into EPC cells, replication of viral components in the nucleus, aggregation and assembly of virus in the cytoplasm and budding release of virus. These steps in the GSIV replication process were sequential.

Entry of GSIV into EPC Cells. At 1 hpi, the GSIV entered EPC cells by endocytosis or fusion after adsorption to the cell membrane. Electron micrographs of EPC cells infected with GSIV and fixed immediately after 1 h showed the enveloped, naked virions and the empty capsid without viral nucleoid adsorbed to the cell membrane or close to coated pits (Figs. 2a–c). Fusion between the viral envelope and the cell membrane was first noted at 1 hpi

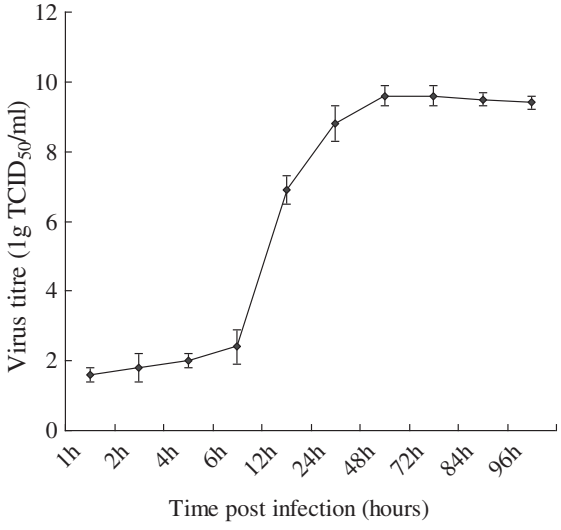

Fig. 1. Growth curve of GSIV in EPC cells.

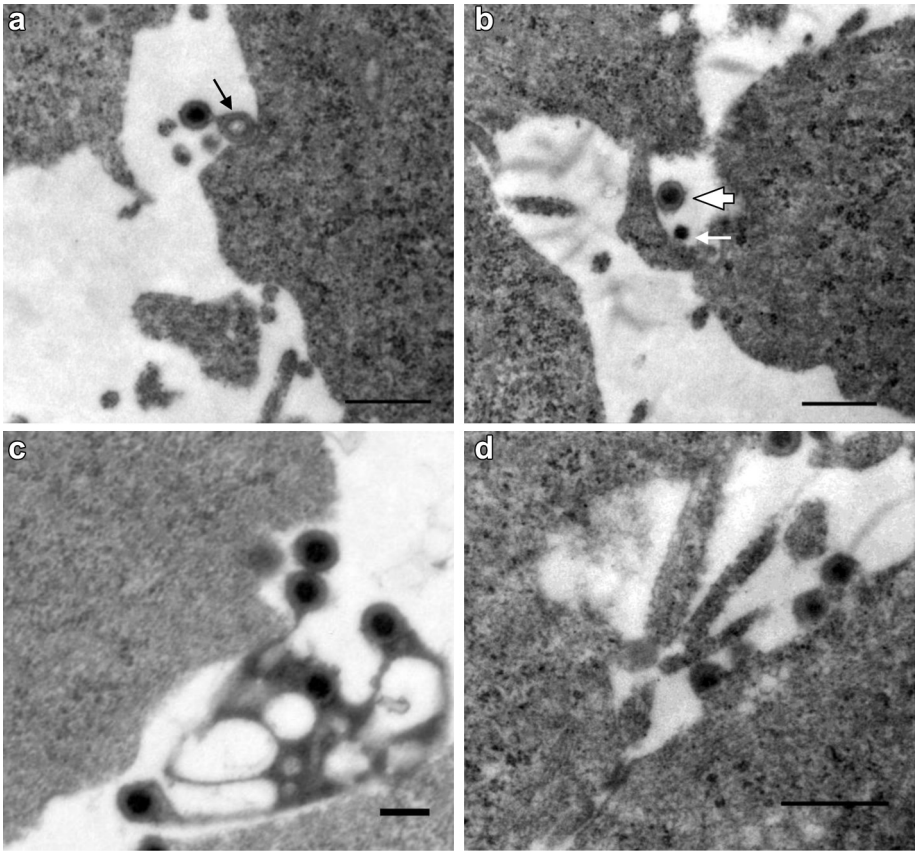

Fig. 2. Entry of GSIV into EPC cells at 1 hpi. (a) The empty capsid without viral nucleoid adsorbed to a cell membrane (arrow). Bar, 500 nm. (b) Enveloped virions (arrowhead) and the naked virions (arrow) adsorbed to a cell membrane. Bar, 500 nm. (c) Some enveloped virions enter EPC cells by endocytosis. Bar, 200 nm. (d) Fusion between the viral capsid and the cell membrane. Bar, 500 nm.

(Fig. 2d). Later, GSIV virions were found deeper inside the cell.

Replication of Viral Components in the Nucleus. Following uncoating, viral cores were released and transported to the host cell nucleus (Fig. 3a), following which viral components were synthesized in the nucleus.

Assembly of Viral Components in the Cytoplasm. The assembly of viral components in the cytoplasm began with the transport of newly-synthesized viral DNA into the cytoplasm. During the course of virus replication, the different stages of virus self-assembly were observed in the cytoplasm (Figs. 3a–d). A slightly electron-lucent viromatrix (morphologically distinct viral assembly site) near the cell nucleus was detected in the virus-infected cells (Figs. 3a–d). Ultrastructural observation showed that GSIV assembled in the viromatrix, which contained large numbers of virus particles in different stages of assembly including partially formed capsids, empty capsids, capsids with partial core and fully mature nucleocapsids (Fig. 3b). Swollen and empty mitochondria was detected around the viromatrix (Fig. 3d) Increased numbers of virions with a dense nucleoid were found scattered throughout the cytoplasm of infected cells after 6 hpi.

Aggregation and Budding Release of GSIV. In the late phase of virus infection (12–24 hpi), most nucleocapsids were formed and clustered in pseudocrystalline arrays in the viromatrix or were budding at the plasma membrane (Fig. 4a). Intracellular particles were wrapped by cellular membrane or tubules and also budded through the plasma membrane (Fig. 4d). The presence of two or three crystalline aggregates of viruses was common (Fig. 4b).

Cell Damage. In the later stage of infection (24–48 hpi), most virions remained within the cell (Fig. 5a) and were only released following lysis of infected cells. The cell damage appeared as vacuolation, swollen and empty mitochondria and karyolysis. Some infected cells were completely lyzed (Figs. 5b, c). Aggregates of virus particles and cell debris were observed between 24 and 48 hpi (Fig. 5d).

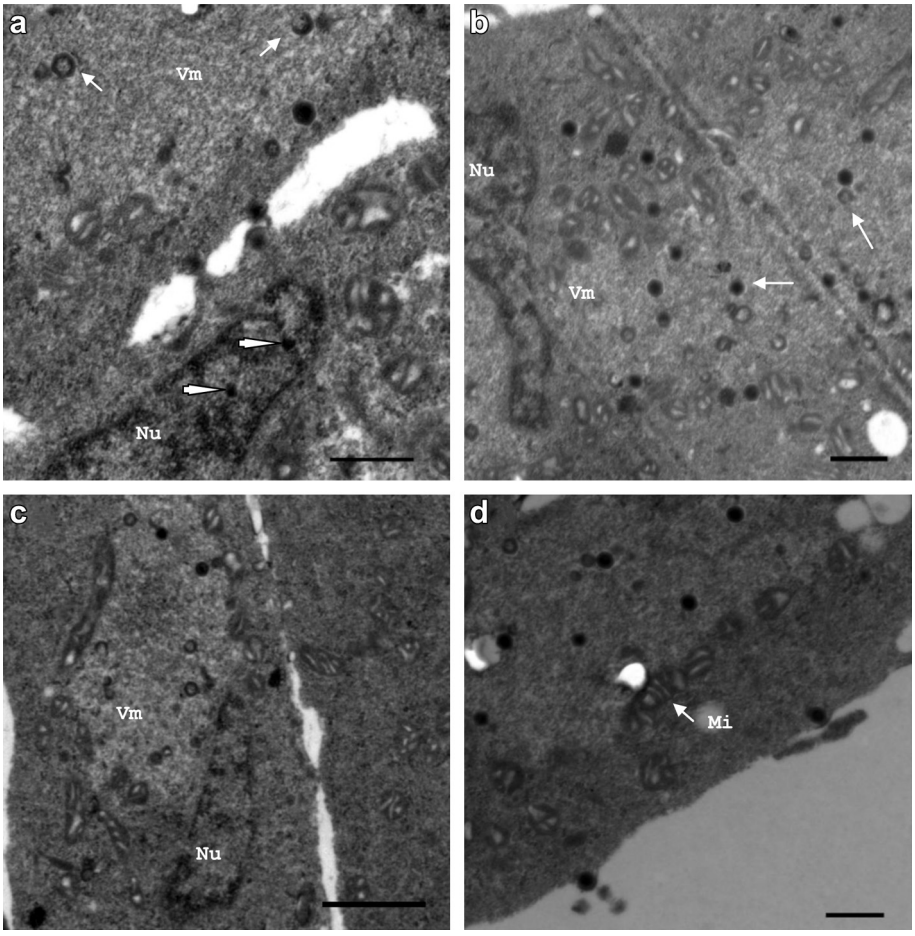

Fig. 3. Assembly of viral components in the infected cells. (a) Viral cores (arrowhead) were released and transported to the host cell nucleus. Empty capsids (arrowed); Nu, Nucleus; Vm, Viromatrix. Bar, 500 nm. (b) Different stages of virus self-assembly in the cytoplasm, including partially formed capsids, empty capsids, capsids with partial core and the fully mature nucleocapsids (arrows). Bar, 500 nm. (c) The viromatrix near the cell nucleus. Bar, 1 μm. (d) Swollen and empty mitochondria (Mi; arrow). Bar, 500 nm.

Discussion

Understanding cellular entry and morphological assembly of virions is important for studying host–virus interactions and developing possible therapeutic strategies against virus infection (Perera *et al.*, 2008; Rodríguez-Cariño *et al.*, 2011). To this end, the interactions between cells and GSIV were examined in an infected fish cell line. A growth curve was produced to examine GSIV propagation in EPC cells to establish the best time to sample the cells for the morphogenesis study. The highest viral titre was at 48 hpi after an eclipse period of about 6 h. A full cytopathic effect was observed in the cell cultures at 2–3 days post infection.

Different stages of GSIV infection, including adsorption, assembly, maturation and budding, were observed in the ultrathin sections of infected cells. After 1 h of adsorption, all of the viral particles, enveloped or naked, had entered the cell. Therefore, with this virus, the presence of an envelope is not a critical requirement for virus infection. This observation helps explain why the titre of GSIV was not affected by freeze–thaw treatment (Gao *et al.*, 2012). The viral envelope is derived in most cases from the cytoplasmic membrane. Enveloped GSIV appears to be internalized via coated pits and then to move through coated vesicles. These morphological results suggest that enveloped GSIV is taken up by a mechanism related to receptor-mediated endocytosis, which occurs via clathrin-coated pits and vesicles (Goldstein *et al.*, 1979; Braunwald *et al.*, 1985). The most frequently observed interaction between naked GSIV and the plasma membrane was fusion, which leads to the incorporation of the virus capsid into the cell membrane. This ability of virus to fuse with cell membranes has also been shown for other members of the family Iridoviridae (Gendrault *et al.*, 1981; Braunwald *et al.*, 1985). Following uncoating, DNA cores are translocated to the nuclear membrane

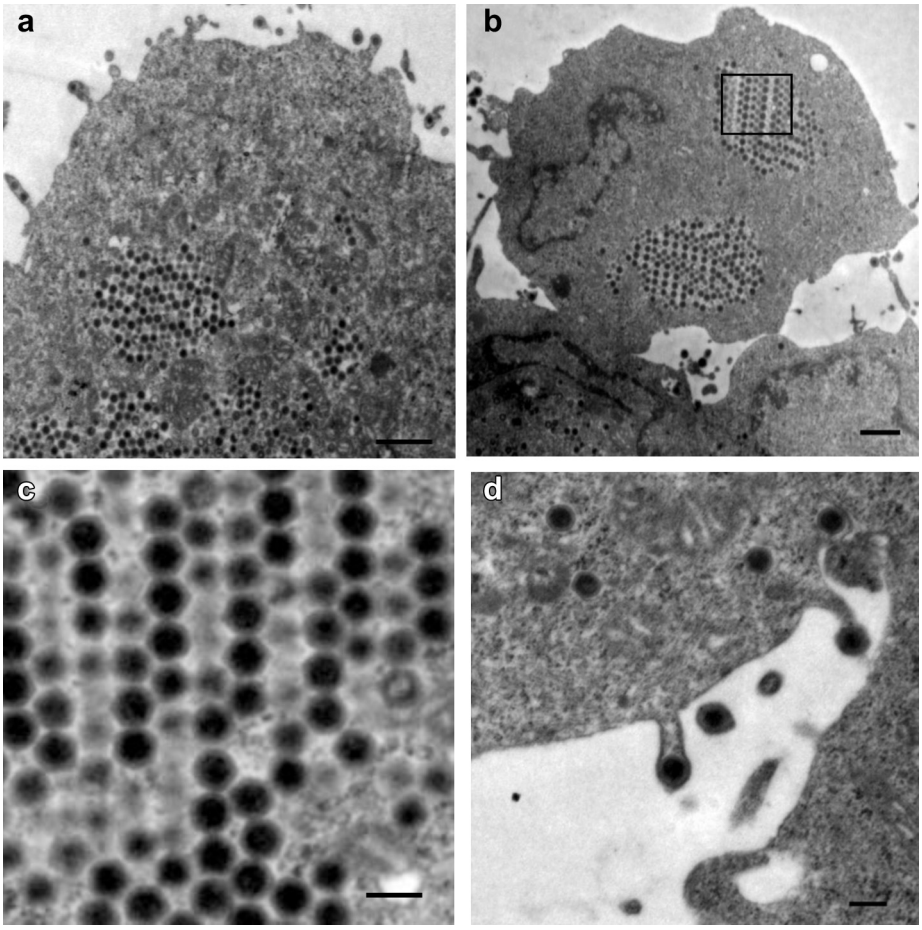

Fig. 4. Mature GSIV 12–24 hpi. (a) Paracrystalline array of non-enveloped virus particles and budding at the plasma membrane. Bar, 1 μm. (b) Two viromatrix areas in the same cell. Bar, 1 μm. (c) High magnification of the region indicated in (b). Bar, 200 nm. (d) Budding from the plasma membrane. Bar, 200 nm.

where they are likely imported into the nucleus via host-encoded nuclear transport mechanisms. Based on the observed frequency of budding, this mechanism seems to be the predominant means by which GSIV exits the cell, at least in the present culture conditions using the EPC cell line.

Cytopathic effect of EPC cells was detected by light microscopy only at 48 hpi, although progeny virus was detected at 12 hpi. This finding highlights the fact that virus infection can be detected readily by electron microscopy early in the course of infection, before cytopathic effect becomes visible. This observation also indicates that cytopathic effect appeared only after extensive damage to the host cells by the virus. Virus exiting through the plasma membrane and associated membrane pinching likely contributes most of the damage, as has been shown for alphavirus (Glasgow *et al.*, 1998). Both the growth curve and the morphology of GSIV were similar to those described previously for other iridoviruses from fish and amphibians (Granzow *et al.*, 1997; Watson *et al.*, 1998; Zhang *et al.*, 1999; Hyatt *et al.*, 2000; Qin *et al.*, 2001).

The family Iridoviridae comprises five genera: *Iridovirus*, *Chloriridovirus*, *Ranavirus* (frog virus [FV] 3 and related agents), *Lymphocystivirus* (lymphocystis disease virus, LDV) and *Megalocytivirus*. Iridoviruses are well-known pathogens of amphibians, fish and insects (King *et al.*, 2011). There are few studies of the infection cycle of iridoviruses (Granzow *et al.*, 1997; Zhang *et al.*, 1999; Qin *et al.*, 2001). Most knowledge of iridovirus replication is based on studies of FV3 from the genus *Ranavirus* (Chinchar, 2002). A comparison of the morphogenesis of GSIV to other iridoviruses shows some shared characteristics, such as the symmetrical shape of the virions, replication cycles involving both nuclear and cytoplasmic phases, budding release from cellular membrane and paracrystalline aggregate formation in cytoplasm. The aquatic animal iridoviruses have been found worldwide, including China, Australia, USA, Venezuela, France, Germany, England, Finland, Japan and Thailand (King *et al.*, 2011). Many iridoviruses had been identified as associated with lethal disease

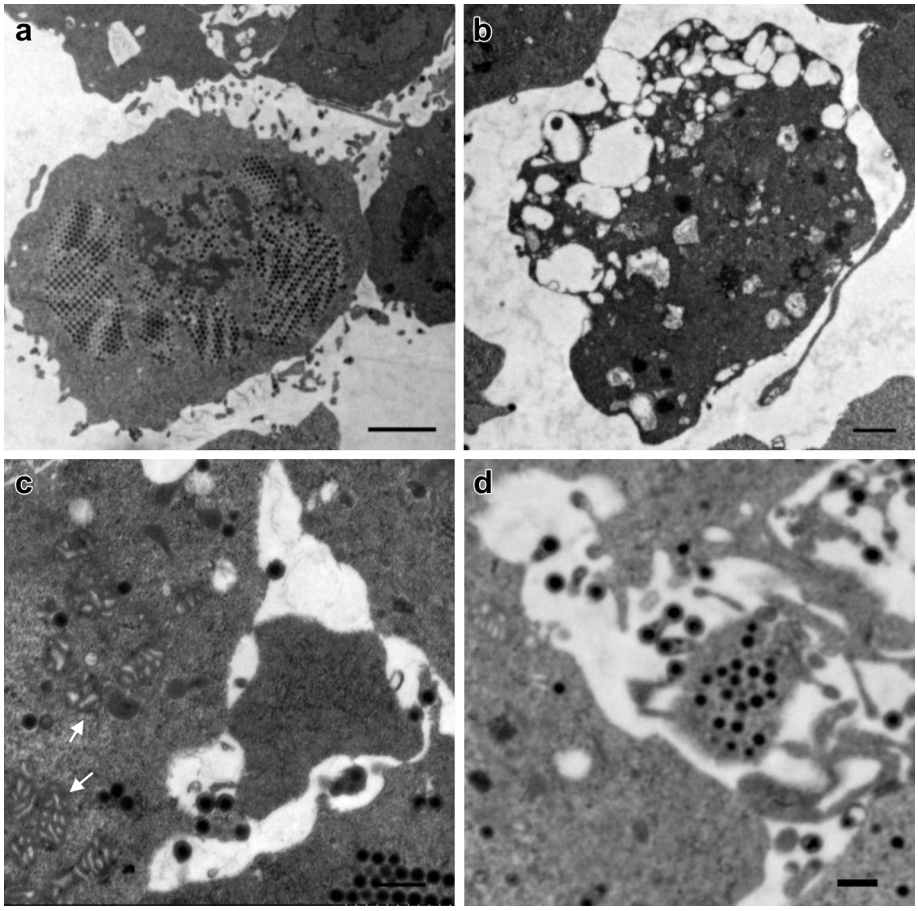

Fig. 5. Types of cell damage at 24–48 hpi. (a) Karyolysis with most virions remaining cell-associated. Virions were only released following lysis of infected cells. Bar, 2 μm. (b) Cell lysis. Bar, 1 μm. (c) Swollen and empty mitochondria (arrows). Bar, 500 nm. (d) Membrane-enclosed aggregates of virus particles with cell debris after cell lysis. Bar, 200 nm.

of aquaculture animals (Moody and Owens, 1994; Ahne *et al*., 1997). The addition of a new iridovirus isolated from the CGS provides more chance to understand the epizootiology of these viruses. Future studies will focus on the development of molecular methods to compare GSIV with other amphibian and fish iridoviruses.

Better understanding the morphogenesis of GSIV will not only help in identification and classification of the viral pathogen, but will also facilitate the development of rapid diagnostic techniques and effective vaccines for the control of this viral disease in aquaculture. Although the EPC cell line is highly permissive to GSIV with high-yield virus production, there remains a requirement to establish a permissive CGS cell line.

Acknowledgements

This study was supported by the Special Fund for Agro-scientific Research in the Public Interest (201203086).

References

Ahne W, Bremont M, Hedrick RP, Hyatt AD, Whittington RJ (1997) Iridoviruses associated with epizootic haematopoietic necrosis EHN in aquaculture. *World Journal of Microbiology and Biotechnology*, **13**, 367–373.

Alves de Matos AP, Paperna I (1993) Ultrastructure of erythrocytic virus of the South African anuran *Ptychadena anchietae*. *Diseases of Aquatic Organisms*, **16**, 105–109.

Braunwald J, Nonnenmacher H, Tripier-Darcy F (1985) Ultrastructural and biochemical study of frog virus 3 uptake by BHK-21 cells. *Journal of General Virology*, **66**, 283–293.

Chinchar VG (2002) Ranaviruses (family Iridoviridae): emerging cold-blooded killers. *Archives of Virology*, **147**, 447–470.

Cunningham AA, Langton TE, Bennett PM, Drury SE, Gough RE *et al*. (1993) Unusual mortality associated with poxvirus-like particles in frogs *Rana temporaria*. *Veterinary Record*, **133**, 141–142.

Drury SE, Gough RE, Cunningham AA (1995) Isolation of an iridovirus-like agent from common frogs (*Rana temporaria*). *Veterinary Record*, **137**, 72–73.

Essani K, Granoff A (1989) Properties of amphibian and piscine iridoviruses: a comparison. In: *Viruses of Lower Vertebrates*, W Ahne, Ed., Springer-Verlag, Berlin, pp. 79–85.

Fijan N, Sulimanoic D, Berzotti M, Muzinic D, Zwillenberg LD *et al*. (1983) Some properties of the epithelioma papulosum cyprini (EPC) cell line from carp *Cyprinus carpio*. *Annales Virologie*, **134**, 203–220.

Furukawa T, Fioretti A, Plotkin S (1973) Growth characteristics of cytomegalovirus in human fibroblasts with demonstration of protein synthesis early in viral replication. *Journal of Virology*, **11**, 991–997.

Gao ZY, Zeng LB, Xiao HB, Zhang H, Meng Y *et al*. (2012) Studies on the physical, chemical and biological characteristics of giant salamander iridovirus. *Freshwater Fisheries*, **42**, 17–26.

Gendrault JL, Steffan AM, Bingen A, Kirn A (1981) Penetration and uncoating of frog virus 3 in cultured rat Kupffer cells. *Virology*, **112**, 375–384.

Geng Y, Wang KY, Zhou ZY, Li CW, Wang J *et al*. (2010) First report of a Ranavirus associated with morbidity and mortality in farmed Chinese giant salamanders (*Andrias davidianus*). *Journal of Comparative Pathology*, **145**, 95–102.

Glasgow GM, McGee MM, Tarbatt CJ, Mooney DA, Sheahan BJ *et al*. (1998) The Semliki Forest virus vector induces p53-independent apoptosis. *Journal of General Virology*, **79**, 2405–2410.

Goldstein JL, Anderson RG, Brown MS (1979) Coated pits, coated vesicles, and receptor-mediated endocytosis. *Nature*, **279**, 678–685.

Granzow H, Weiland F, Fichtner D, Enzmann PJ (1997) Studies of the ultrastructure and morphogenesis of fish pathogenic viruses grown in cell culture. *Journal of Fish Diseases*, **20**, 1–10.

Hedrick RP, McDowell TS (1995) Properties of iridoviruses from ornamental fish. *Veterinary Record*, **26**, 423–427.

Hedrick RP, Mcdowell TS, Ahne W, Torhy C, de Kinkelin P (1992) Properties of three iridoviruses-like agents associated with systemic infections of fish. *Diseases of Aquatic Organisms*, **13**, 203–209.

Hengstberger SG, Hyatt AD, Speare R, Coupar BEH (1993) Comparison of epizootic haematopoietic necrosis and Bohle iridoviruses, recently isolated Australian iridoviruses. *Diseases of Aquatic Organisms*, **15**, 93–107.

Hyatt AD, Gould AR, Zupanovic Z, Cunningham AA, Hengstberger S *et al*. (2000) Comparative studies of piscine and amphibian iridoviruses. *Archives of Virology*, **145**, 301–331.

Jiang YL, Zhang M, Jing HL, Gao LY (2011) Isolation and characterization of an Iridovirus from sick giant salamander (*Andrias davidianus*). *Bing Du Xue Bao*, **27**, 274–282.

King AMQ, Adams MJ, Carstens EB, Lefkowitz EJ (2011) *Virus Taxonomy: Ninth Report of the International Committee on Taxonomy of Viruses*. EA Press, London, pp. 193–194.

Moody NJG, Owens L (1994) Experimental demonstration of the pathogenicity of a frog virus, Bohle iridovirus, for a fish species, *Barramundi Lates calcarifer*. *Diseases of Aquatic Organisms*, **18**, 95–102.

Perera R, Khaliq M, Kuhn RJ (2008) Closing the door on flaviviruses: entry as a target for antiviral drug design. *Antiviral Research*, **80**, 11–22.

Qin QW, Lam TJ, Sin YM, Shen H, Chang SF *et al*. (2001) Electron microscopic observations of a marine fish iridovirus isolated from brown-spotted grouper, *Epinephelus tauvina*. *Journal of Virological Methods*, **98**, 17–24.

Reed LJ, Muench H (1938) A simple method of estimating fifty percent end points. *American Journal of Epidemiology*, **27**, 493–497.

Rodríguez-Cariño C, Duffy C, Sánchez-Chardi A, McNeilly F, Allan GM *et al*. (2011) Porcine circovirus type 2 morphogenesis in a clone derived from the l35 lymphoblastoid cell line. *Journal of Comparative Pathology*, **144**, 91–102.

Wang XM, Zhang KJ, Wang ZH, Ding YZ, Wu W *et al*. (2004) The decline of the Chinese giant salamander *Andrias davidianus* and implications for its conservation. *Oryx*, **38**, 197–202.

Watson LR, Groff JM, Hedrick RP (1998) Replication and pathogenesis of white sturgeon iridovirus WSIV in experimentally infected white sturgeon *Acipenser transmontanus* juveniles and sturgeon cell lines. *Diseases of Aquatic Organisms*, **32**, 173–184.

Zhang QY, Li ZQ, Gui JF (1999) Studies on morphogenesis and cellular interactions of Rana grylio virus (RGV) in an infected fish cell line. *Aquaculture*, **175**, 185–197.

Zhang QY, Xiao F, Gui JF, Mao J, Chinchar VG (2001) Characterization of an iridovirus from the cultured pig frog, *Rana grylio*, with a lethal syndrome. *Diseases of Aquatic Organisms*, **48**, 27–36.

Zhou Y, Zeng LB, Meng Y, Zhou QL, Zhang H *et al*. (2012) Establishment of a TaqMan real-time PCR assay for detecting the giant salamander iridovirus. *Journal of the Fisheries of China*, **36**, 772–778.

Zupanovic Z, Musso C, Lopez G, Louriero CL, Hyatt AD *et al*. (1998) Isolation and characterization of iridoviruses from the giant toad *Bufo marinus* in Venezuela. *Diseases of Aquatic Organisms*, **33**, 1–9.

[*Received, June 1st, 2013*
Accepted, September 19th, 2013]